Pressure dependent effect of hydrogen adsorption on structural and electronic properties of Pt/γ-Al_2O_3 nanoparticles

H. Mistry[1], F. Behafarid[1], Simon R. Bare[2], B. Roldan Cuenya[1,3*]

[1]Department of Physics, University of Central Florida, Orlando, FL 32816

[2]UOP LLC, a Honeywell Company, Des Plaines, IL 60017

[3]Department of Physics, Ruhr University Bochum, Bochum, Germany

*roldan@ucf.edu; Beatriz.Roldan@rub.de

Table of Contents Entry

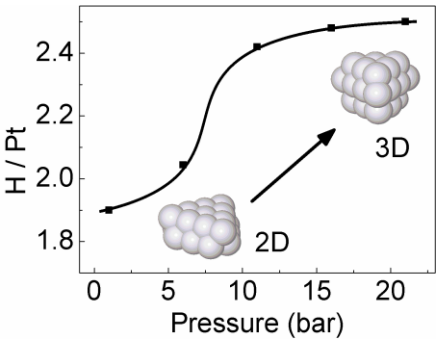

Using *in-situ* X-ray absorption fine structure spectroscopy, a striking 2D to a 3D shape transformation is revealed in size- and shape-controlled Pt/γ-Al_2O_3 nanoparticles under increasing H_2 pressure at room temperature. In addition, the ability of these particles to adsorb up to 2.5 hydrogen per platinum atom is demonstrated.

Abstract

Understanding the interaction of hydrogen with subnanometer platinum nanoparticles (NPs) under industrially relevant conditions is of great importance to heterogeneous catalysis. In this work, we investigate the pressure dependent changes in hydrogen coverage on size- and shape-selected Pt/γ-Al_2O_3 NPs using *in situ* XANES measurements. ΔXANES calculations revealed an increase in H/Pt ratio from 1.9 to 2.5 by increasing the hydrogen pressure from 1 bar to 21 bar at room temperature. In addition, EXAFS measurements of the local geometrical structure showed changes in Pt-Pt bond length and coordination number, revealing a morphological transformation in the NPs from a 2D to a 3D shape under increasing H_2 pressure at room temperature. Such

shape evolution leads to a decrease in the NP-support contact area and is thus expected to affect the NP stability against coarsening.

Keywords: Pt nanoparticle, Al_2O_3, hydrogen, XANES, EXAFS, pressure, shape transformation.

Introduction

The interaction of hydrogen with supported noble metal nanoparticles (NPs) is of great interest in heterogeneous catalysis, especially for applications such as hydrogenation reactions,[1] electrocatalysis,[2] and hydrogen storage.[3] Recent research has shown many of these catalytic processes to be dependent on catalyst particle size and shape.[4] Smaller, subnanometer-sized particles are often more active because of the increased number of edge and corner sites. For some chemical processes, these properties might correspond to the increased ability of such small NPs to adsorb hydrogen,[5] which has received much attention in recent literature, particularly for the Pt/Al_2O_3 system.[6] On Pt(111) single crystals, hydrogen coverage has been measured to saturate at a 1:1 ratio of H/Pt, a fact commonly used to calibrate metallic surface area measurements.[7] However, H_2 chemisorption isotherm measurements have indicated that nanometer-sized particles can adsorb between 1.1 to 1.5 H atoms per Pt.[8] Theoretical work has predicted even higher hydrogen coverages for subnanometer Pt particles,[9] such as Pt_{13} NPs which can stabilize 3.3 H/Pt due to a particle shape reconstruction.[6c] Using size- and shape-selected $Pt/\gamma\text{-}Al_2O_3$ NPs, Behafarid et al.[6a] observed experimentally that small NPs with a large number of low-coordinated surface atoms (corner and edge sites) can adsorb significantly more H/Pt at atmospheric pressure than larger, more bulk-like NPs.

Understanding the adsorption of hydrogen on NP surfaces has been challenging because of the complex interplay between particle structure and electronic properties, adsorbate interactions, and support effects.[6a, 10] Furthermore, under realistic reaction pressures and temperatures, NPs can have a dynamic structure which allows them to transition between several stable structural isomers,[6c, 11] which further complicates their characterization. Several recent studies have measured morphological changes in Pt NPs under hydrogen environments.[8c, 12] Particularly interesting are recent theoretical investigations by Mager-Maury et al.,[6c] who calculated structural changes in subnanometer $Pt/\gamma\text{-}Al_2O_3$ NPs as a function of temperature and pressure. Their theoretical work predicts that an increase in the H coverage should result in Pt_{13} NPs to evolve from a biplanar to a cuboctahedral morphology due to a weakened metal-support interaction and *surface* Pt hydride formation. [6c]

In situ X-ray absorption near-edge structure (XANES) spectroscopy at the Pt-L_3 edge has proved to be an excellent tool for the study of hydrogen adsorption on Pt NPs through observing

changes in the *d* electron density of the particles under different adsorbate environments.[6a, 8c, 10b, c, 12a, 13] In this experimental work we investigate the pressure-dependent changes in hydrogen coverage on size- and shape-selected Pt/γ-Al_2O_3 NPs as well as on their structure using *in-situ* XANES and EXAFS measurements. ΔXANES plots were used to quantify the H/Pt ratio as a function of H_2 pressure. In addition, EXAFS measurements showed changes in Pt-Pt bond length and coordination number, revealing morphology changes in the Pt NPs at room temperature under increasing H_2 pressure.

Results and discussion

The Pt L_3-edge XANES of size-selected 0.8 ± 0.2 nm Pt NPs with 2D shape[14] were measured as a function of H_2 pressure. Figure 1 shows the normalized absorption coefficient of Pt NPs acquired in a H_2 pressure of 1 to 21 bar and in 1 bar He at 25°C. A positive shift (+0.6 eV) in the absorption edge energy was observed upon hydrogen chemisorption as compared to the foil. Additionally, the intensity of the absorption peak (white line, WL) was found to increase with increasing H_2 pressure, with adsorbate-free NPs measured in He showing a significantly lower intensity. The white line intensity corresponds to the unoccupied *5d* electron density of states, and its increase upon hydrogen adsorption reflects the transfer of charge from Pt to H. Furthermore, a broadening of the WL is observed upon hydrogen chemisorption. As shown in Refs. [6a, 13b, 13d, 15], the area of the absorption peak can be used to extract quantitative information on the hydrogen coverage on the NPs. However, in order to conduct such analysis, a reference of the hydrogen-free state of the NPs is required. For this purpose, XANES data obtained in helium were used here as reference. To ensure that the Pt NPs were hydrogen free during measurement in helium, the reaction cell was pressurized to 4 bar He and heated to 375°C for 30 minutes, then cooled to 25°C before the measurement. An alternative approach involves the use of reference XANES data acquired under hydrogen at a high enough temperature where negligible amounts of hydrogen would be adsorbed on the NP surface (375°C for our Pt_{22} NPs, as shown in Suppl. Fig. S2).

In order to quantify the change in the hydrogen coverage on the NP surface under elevated H_2 pressure at 25°C, ΔXANES plots were calculated. Figure 2(a) shows the ΔXANES spectra for Pt NPs measured in 1-21 bar H_2 at 25°C. An increase in the area of peak B is seen with an increase in H_2 pressure, corresponding to an increase in H coverage on the NP surface. To

estimate H/Pt ratios, the area of the ΔXANES peak B was normalized by the peak B area of largee 1 nm diameter particles (Pt_{140}) with well-defined shape previously measured[6a] in 1 bar H_2 at 183 K. Under these conditions, the larger NPs (Pt_{140}) are postulated to be saturated with one hydrogen atom per surface platinum atom. The number of hydrogen atoms per total number of Pt atoms in the Pt_{22} NP are shown in Fig. 2(b). To best compare our H/Pt ratios with those found in the literature, we have normalized the hydrogen coverage by the total number of atoms in the NP, and not the number of Pt atoms at the surface, as was given in our previous work.[6a] The hydrogen coverage on the NPs at 25°C was found to increase from 1.9 to 2.5 H/Pt with an increase of pressure from 1 to 21 bar. Theoretical (DFT) H/Pt ratios for Pt_{13} NPs calculated by Mager-Maury et al.[6c] are also plotted in Figure 2(b). For these smaller NPs, a higher H/Pt ratio of ~2.6 is seen at atmospheric pressure of H_2, which increases only slightly with increasing H_2 pressure. This indicates that their smaller theoretical Pt_{13} NPs able to adsorb more H_2 than our experimental Pt_{22} NPs under equivalent conditions.,This trend is in agreement with our previous work on Pt/γ-Al_2O_3 NPs showing that hydrogen adsorption capacity increases with decreasing particle size.[6a] Similarly, Jensen et al.[12b] obtained a saturation coverage of 2.9 H/Pt at 25°C for their smaller Pt_{13} NPs supported on a zeolite using H adsorption isotherms.

In order to investigate any morphological changes in the Pt NPs with increasing hydrogen coverage, EXAFS analysis was performed to extract coordination number (1st nearest neighbor CN, NN1) and bond length (R) information as a function of the hydrogen pressure. All EXAFS data from the reduced Pt NPs were fitted with two components corresponding to Pt-Pt (2.76 Å) and a long Pt-O (~2.5 Å) bond.[4d, 16] The Pt-O component has a longer bond length than that of Pt oxide species or chemisorbed oxygen on Pt (~2.0 Å), and is assigned to the NP/support interface.[4d, 16] The magnitude of the Fourier transform EXAFS data acquired in hydrogen at 25°C from 1 bar to 21 bar are shown in Figure 3 together with an example fit as inset. The rest of the 1st nearest neighbor fits are shown in Suppl. Figs. S3-S7. Table 1 shows EXAFS results for the Pt-Pt and Pt-O first shell fits. Figure 4 displays (a) Pt-Pt 1st nearest neighbor CNs (NN1) and (b) Pt-Pt bond distances for our Pt NPs under increasing H_2 pressure extracted from the analysis of EXAFS data. Included in (a) are also NN1 data for Pt_{13} clusters from Mager-Maury et al.[6c] as a function of the H/Pt ratio.

Our results reveal that an increase in H_2 pressure correlates to an increase in NN1 from 7.5 to 8.8, which indicates a structural change in the NPs as H adsorption increases. A significant

change in Pt-Pt coordination number occurs between 16 and 21 bar, indicating a possible abrupt structural change at this pressure. The Pt-Pt 1st nearest neighbor distance shows a slight increase with H_2 pressure up to 21 bar, at which point it drops. Pt-O CN decreases with increasing hydrogen pressure, indicating that Pt-O bonds between the metal and the hydroxylated Al_2O_3 support are broken. The increase in Pt-Pt CN and bond distance, together with a concomitant decrease in the Pt-O CN, suggest that the NPs are restructured from their original 2D bilayer shape, modeled by our shape analysis,[6a, 14] to a more 3D-like structure upon hydrogen adsorption.

Previous theoretical studies have predicted hydrogen-induced morphological changes in subnanometer Pt NPs. For example, calculations by Mager-Maury et al.[6c] on Pt_{13} clusters supported on γ-Al_2O_3 revealed that they are stabilized in a 2D biplanar configuration at low hydrogen coverage due to strong metal-support interactions. However, at coverages above ~1.5 H/Pt, these NPs are transformed to a 3D cubocahedral shape due to a weakening of the metal-support interaction by the adsorbed H, which is believed to accumulate at the NP/support interface and to contribute to NP/support bond breaking. A transformation from 2D to 3D shape would explain the increasing Pt-Pt CN with increasing H_2 pressure seen in this study, and also the drop in Pt-O CN as bonds between metal and support are broken. It should be, however, noted in Fig. 4(a) that the calculations in Ref. [6c] showed a roughly constant cuboctahedral shape for the high H/Pt coverages used in our study, since their Pt_{13} NPs have already undergone a shape transformation from biplanar to cuboctahedral shape. It is plausible that their smaller Pt_{13} NPs are more susceptible to shape transformation at lower H coverages due to their smaller size. Sintering could be another possible explanation for the increase in the Pt-Pt CN. Room temperature Ostwald ripening has been reported for Pd nanoclusters upon exposure to hydrogen, which was explained by the formation of Pd hydride.[17] Subsurface absorption of hydrogen would result in a decrease in Pt-Pt coordination numbers, which was not observed in this study. Therefore, room temperature NP growth is not likely to occur in our samples, since they were also already pre-annealed in H_2 at much higher temperature (375°C) without any evidence of sintering.[14b] While our results show no evidence for subsurface hydrogen, surface hydride species may still form on our NPs. While Pt NPs are not known to form hydrides, Hakamada et al. [18] reported that nanoporous Pt could form hydride species under lattice strain.[18] In addition,

theoretical studies predict the formation of Pt hydrides on nanoparticles at high H coverage.[6c, 11b]

Recent work by Jensen et al.[12b] has shown experimental evidence for Pt NPs restructuring under hydrogen pressure. Their Pt_{13}/KL zeolite NPs were measured by EXAFS after reduction in H_2 and after H desorption by heating at 573 K. Upon desorbing H, the Pt-Pt CN decreases, Pt-O CN increases, and the Pt-Pt bond distance decreases, which the authors attribute to a restructuring of the NP to a flatter shape with more support interaction. DFT calculations by Chen et al.[11b] also predicted restructuring for unsupported Pt_{13} NPs, which undergo a phase transformation from icosahedral to fcc structure at ~0.8 H/Pt, and above 2.8 H/Pt, H atoms can penetrate into the structure.

In our study, the Pt-Pt bond distance shown in Figure 4(b) increases with increasing hydrogen pressure until a coverage of 2.5 H/Pt is reached, at which point the bond distance drops. For nanometer-sized Pt NPs, the Pt-Pt bond distance has been shown to increase with increasing hydrogen coverage due to lifting of the bond length contraction by the adsorbed hydrogen.[8c, 10c, 12a, 19] A structural change in the NPs to a more 3D shape with a lower fraction of atoms at the surface would also relieve surface strain responsible for bond contraction. The anomalous drop in bond distance measured at the highest pressure does not fit the previously described trends, but might be plausible if the strain induced by the NP-support is initially expansive, in which case the NP break off from the support would result in Pt-Pt bond length contraction. Indeed, DFT calculations by Hu et al.[10a] predict that for the majority of stable Pt_{13} cluster shapes, the γ-Al_2O_3 support induces an expansion in the Pt-Pt distance as compared to unsupported NPs. Alternatively, this drop could be related to decomposition of surface hydride species at high hydrogen pressures, which was seen on nanoporous Pt above 13 bar H_2 pressure.[18] Nevertheless, it should be noted that since no loss of hydrogen was observed at this pressure via XANES, the latter possibility is unlikely.

The present work illustrates the intricate correlation between the nanoparticle environment (surrounding adsorbates and support) and the electronic and structural characteristics of small NPs. In order to gain further insight into these effects, additional studies are planned with Pt NPs of different size and shape, and to extend the H_2 pressure regime to higher values.

Conclusions

An *in situ* investigation of the role of chemisorbed hydrogen on the electronic and structural properties of size-controlled Pt NPs supported on γ-Al_2O_3 was carried out via XANES and EXAFS. *In situ* XANES measurements on ~0.8 nm Pt NPs (Pt_{22}) revealed an increase in the hydrogen coverage on the surface of the NPs (H/Pt ratio) with increasing hydrogen pressure from 1 to 21 bar at 25°C. Furthermore, EXAFS measurements revealed a change in the structure of the NPs from 2D to 3D, evidenced by increasing Pt-Pt CNs and decreasing Pt-O (NP/support interface) coordination numbers. This study highlights the dynamic nature of NP catalysts under industrially relevant conditions and the superior adsorption capacity of subnanometer particles, properties which have high importance to catalyst design.

Experimental Methods

Pt/γ-Al_2O_3 NPs were prepared in solution via inverse micelle encapsulation. A PS-b-P2VP diblock copolymer was dissolved in toluene to create micellar cages, which were then loaded with Pt by adding H_2PtCl_6 to the solution and stirring for 2 days. The molar ratio of Pt to polymer P2VP was 0.05. The solution was then filtered, nanocrystalline γ-Al_2O_3 powder (average grain size 40 nm) was added, and then the solution was stir-dried in air at 60°C. The Pt/γ-Al_2O_3 NPs were then calcined at 375°C in O_2 for 24 hours to remove the polymer, and X-ray photoelectron spectroscopy was used to demonstrate that the encapsulating polymers were completely removed, as indicated by the absence of a C 1s signal. The size and shape of the prepared NPs was determined using a combination of low temperature EXAFS multiple scattering analysis and TEM diameter measurements. Details on the shape analysis are given in the Suppl. Figure S1. The above synthesis resulted in a narrow size distribution (size-selected) (0.8 ± 0.2 nm) Pt NPs with approximately 22 atoms (Pt_{22}) in a flat (2D) bilayer shape.[14]

XAFS measurements were performed at Beamline 10-ID-B of the Advanced Photon Source at Argonne National Laboratory. 60 mg of the Pt/γ-Al_2O_3 sample was loaded into an *in situ* high pressure reaction cell allowing pressurization above 20 bars.[20] The reaction cell was housed within a furnace allowing for sample heating via an external PID temperature controller. The Pt L_3 edge was measured in transmission mode, and at least three spectra were acquired at each pressure condition for signal averaging. The gas flows were controlled using Brooks mass flow controllers. The sample was first reduced in 50% H_2 balanced by He at a flow of 50 mL/min at 375°C. Next, the sample was cooled to 25°C and measured at atmospheric pressure in H_2, then

measurements were taken after the cell was pressurized to 6, 11, 16, and 21 bar of H_2. The reactor was then depressurized to 4 bar, flushed with He, and heated to 375°C to remove all H_2 from the sample, and a measurement of the adsorbate free NPs was taken at 25°C in 4 bar He. A final set of measurements was taken at 375°C in H_2 pressures of 0.15, 0.5, and 3 bar.

Data processing was conducted using the IFEFFIT[21] package. Using the Athena software,[22] reference spectra from each measurement were aligned to a Pt reference foil, and then data were merged and normalized by fitting smooth curves to the pre-edge and post-edge. ΔXANES plots were constructed by subtracting the spectra measured in Heat 25°C from spectra measured at various pressures of H_2. Due to the presence of isosbestic points in XANES data at different hydrogen coverages, the ΔXANES data crosses the zero value at the same energies for all different H coverages. The area of the second ΔXANES peak, or the so called peak B[6a] (marked in Fig .2a), was integrated using OriginLab software over the same energy range in which peak B was positive. EXAFS spectra were fit in R-space in the Artemis software[22] with FEFF8 calculations of fcc Pt to simulate Pt-Pt scattering paths and the Pt-O scattering path from $Na_2Pt(OH)_6$ to simulate Pt-O scattering paths. Data sets measured under different pressures were fit simultaneously with the energy shift ΔE_0 constrained, and due to the strong correlation between Pt-Pt coordination number and bond distance disorder (σ^2), σ^2 was fit as a shared parameter. Additional fit details and example fits are given in the Suppl. documents.

Acknowledgment

The support of Prof. Carlo Segre from the Illinois Institute of Technology setting up the XAFS beamline at ANL is greatly appreciated. In addition, the authors are grateful to Lindsay Merte, Estephania Lira, and Sudeep Pandey for their assistance with the EXAFS measurements. This work was funded by the Office of Basic Energy Sciences from the US Department of Energy under contract DE-FG02-21 08ER15995.

References

[1] (a) F. Zaera, *Phys. Chem. Chem. Phys.* **2013**; (b) P. Rylander, *Catalytic Hydrogenation over Platinum Metals*, Academic Press, **1967**.

[2] (a) C. Cui, M. Ahmadi, F. Behafarid, L. Gan, M. Neumann, M. Heggen, B. Roldan Cuenya, P. Strasser, *Faraday Discuss.* **2013**; (b) A. Wieckowski, E. R. Savinova, C. G. Vayenas, *Catalysis and Electrocatalysis at Nanoparticle Surfaces*, CRC Press, **2003**.

[3] (a) Y. Li, R. T. Yang, *J. Phys. Chem. C* **2007**, *111*, 11086-11094; (b) L. Wang, R. T. Yang, *J. Phys. Chem. C* **2008**, *112*, 12486-12494.

[4] (a) S. Mukerjee, *J. Appl. Electrochem.* **1990**, *20*, 537-548; (b) M. Yamauchi, H. Kobayashi, H. Kitagawa, *ChemPhysChem* **2009**, *10*, 2566-2576; (c) B. Roldan Cuenya, *Thin Solid Films* **2010**, *518*, 3127-3150; (d) M. Vaarkamp, J. T. Miller, F. S. Modica, D. C. Koningsberger, *J. Catal.* **1996**, *163*, 294-305.

[5] C. Zhou, J. Wu, A. Nie, R. C. Forrey, A. Tachibana, H. Cheng, *J. Phys. Chem. C* **2007**, *111*, 12773-12778.

[6] (a) F. Behafarid, L. Ono, S. Mostafa, J. Croy, G. Shafai, S. Hong, T. Rahman, S. R. Bare, B. Roldan Cuenya, *Phys. Chem. Chem. Phys.* **2012**, *14*, 11766-11779; (b) M. K. Oudenhuijzen, J. A. van Bokhoven, J. T. Miller, D. E. Ramaker, D. C. Koningsberger, *J. Am. Chem. Soc.* **2005**, *127*, 1530-1540; (c) C. Mager-Maury, G. Bonnard, C. Chizallet, P. Sautet, P. Raybaud, *ChemCatChem* **2011**, *3*, 200-207.

[7] L. Spenadel, M. Boudart, *J. Phys. Chem.* **1960**, *64*, 204-207.

[8] (a) B. Kip, F. Duivenvoorden, D. Koningsberger, R. Prins, *J. Catal.* **1987**, *105*, 26-38; (b) J. Singh, R. C. Nelson, B. C. Vicente, S. L. Scott, J. A. van Bokhoven, *Phys. Chem. Chem. Phys.* **2010**, *12*, 5668-5677; (c) E. Bus, J. A. van Bokhoven, *Phys. Chem. Chem. Phys.* **2007**, *9*, 2894-2902.

[9] (a) P. S. Petkov, G. P. Petrova, G. N. Vayssilov, N. Rösch, *J. Phys. Chem. C* **2010**, *114*, 8500-8506; (b) A. Vargas, G. Santarossa, A. Baiker, *J. Phys. Chem. C* **2011**, *115*, 10661-10667; (c) X. Liu, H. Dilger, R. Eichel, J. Kunstmann, E. Roduner, *J. Phys. Chem. B* **2006**, *110*, 2013-2023.

[10] (a) C. H. Hu, C. Chizallet, C. Mager-Maury, M. Corral-Valero, P. Sautet, H. Toulhoat, P. Raybaud, *J. Catal.* **2010**, *274*, 99-110; (b) Y. Lei, J. Jelic, L. C. Nitsche, R. Meyer, J. Miller, *Top. Catal.* **2011**, *54*, 334-348; (c) S. I. Sanchez, L. D. Menard, A. Bram, J. H. Kang, M. W. Small, R. G. Nuzzo, A. I. Frenkel, *J. Am. Chem. Soc.* **2009**, *131*, 7040-7054.

[11] (a) G. Rupprechter, H.-J. Freund, *Top. Catal.* **2000**, *14*, 3-14; (b) L. Chen, C.-g. Zhou, J.-p. Wu, H.-s. Cheng, *Front. Phys. China* **2009**, *4*, 356-366.

[12] (a) M. W. Small, S. I. Sanchez, N. S. Marinkovic, A. I. Frenkel, R. G. Nuzzo, *ACS Nano* **2012**, *6*, 5583-5595; (b) C. Jensen, D. Buck, H. Dilger, M. Bauer, F. Phillipp, E. Roduner, *Chem. Commun.* **2013**, *49*, 588-590.

[13] (a) Y. Ji, V. Koot, A. M. van der Eerden, B. M. Weckhuysen, D. C. Koningsberger, D. E. Ramaker, *J. Catal.* **2007**, *245*, 415-427; (b) N. Guo, B. R. Fingland, W. D. Williams, V. F. Kispersky, J. Jelic, W. N. Delgass, F. H. Ribeiro, R. J. Meyer, J. T. Miller, *Phys. Chem. Chem. Phys.* **2010**, *12*, 5678-5693; (c) O. S. Alexeev, F. Li, M. D. Amiridis, B. C. Gates, *J. Phys. Chem. B* **2005**, *109*, 2338-2349; (d) T. Kubota, K. Asakura, N. Ichikuni, Y. Iwasawa, *Chem. Phys. Lett.* **1996**, *256*, 445-448; (e) D. Ramaker, D. Koningsberger, *Phys. Chem. Chem. Phys.* **2010**, *12*, 5514-5534; (f) S. N. Reifsnyder, M. M. Otten, D. E. Sayers, H. H. Lamb, *J. Phys. Chem. B* **1997**, *101*, 4972-4977; (g) S. Bordiga, E. Groppo, G. Agostini, J. A. van Bokhoven, C. Lamberti, *Chem. Rev.* **2013**, *113*, 1736-1850; (h) M. Teliska, W. O'Grady, D. Ramaker, *J. Phys. Chem. B* **2004**, *108*, 2333-2344.

[14] (a) B. Roldan Cuenya, M. A. Ortigoza, L. Ono, F. Behafarid, S. Mostafa, J. Croy, K. Paredis, G. Shafai, T. Rahman, L. Li, *Phys. Rev. B* **2011**, *84*, 245438; (b) B. Roldan Cuenya, J. R. Croy, S. Mostafa, F. Behafarid, L. Li, Z. Zhang, J. C. Yang, Q. Wang, A. I. Frenkel, *J. Am. Chem. Soc.* **2010**, *132*, 8747-8756.

[15] A. Y. Stakheev, Y. Zhang, A. Ivanov, G. Baeva, D. Ramaker, D. Koningsberger, *J. Phys. Chem. C* **2007**, *111*, 3938-3948.

[16] (a) K. Paredis, L. K. Ono, F. Behafarid, Z. Zhang, J. C. Yang, A. I. Frenkel, B. R. Cuenya, *J. Am. Chem. Soc.* **2011**, *133*, 13455-13464; (b) Y. Zhang, M. L. Toebes, A. van der Eerden, W. E. O'Grady, K. P. de Jong, D. C. Koningsberger, *J. Phys. Chem. B* **2004**, *108*, 18509-18519; (c) A. Y. Stakheev, Y. Zhang, A. Ivanov, G. Baeva, D. Ramaker, D. Koningsberger, *The Journal of Physical Chemistry C* **2007**, *111*, 3938-3948; (d) L. R. Merte, M. Ahmadi, F. Behafarid, L. K. Ono, E. Lira, J. Matos, L. Li, J. C. Yang, B. Roldan Cuenya, *ACS Catal.* **2013**, 130517100016006.

[17] M. Di Vece, D. Grandjean, M. Van Bael, C. Romero, X. Wang, S. Decoster, A. Vantomme, P. Lievens, *Phys. Rev. Lett.* **2008**, *100*.

[18] M. Hakamada, T. Furukawa, T. Yamamoto, M. Takahashi, M. Mabuchi, *Mater. Trans.* **2011**, *52*, 806-809.

[19] E. Bus, J. T. Miller, A. J. Kropf, R. Prins, J. A. van Bokhoven, *Phys. Chem. Chem. Phys.* **2006**, *8*, 3248-3258.

[20] S. R. Bare, N. Yang, S. D. Kelly, G. E. Mickelson, F. S. Modica, *Catal. Today* **2007**, *126*, 18-26.

[21] M. Newville, *J. Synchrotron Radiat.* **2001**, *8*, 322-324.

[22] B. Ravel, M. Newville, *J. Synchrotron Radiat.* **2005**, *12*, 537-541.

H_2 Pressure	NN1 (Pt-Pt)	R (Å) (Pt-Pt)	NN1 (Pt-O)	R (Å) (Pt-O)
0 bar (He)	6.0 (7)	2.733 (5)	2 (1)	2.52 (3)
1 bar	7.5 (7)	2.755 (4)	1.6 (8)	2.50 (4)
6 bar	7.6 (7)	2.755 (4)	1.7 (9)	2.55 (4)
11 bar	8.0 (7)	2.761 (4)	1.5 (8)	2.49 (5)
16 bar	8.0 (7)	2.761 (3)	1.5 (8)	2.49 (4)
21 bar	8.8 (8)	2.752 (3)	0.8 (7)	2.53 (8)

Table 1. First nearest neighbor (NN1) coordination numbers and Pt-Pt and Pt-O bond distances (R) extracted from single scattering analysis of EXAFS data acquired on Pt NPs at 25°C in different pressures of H_2. The EXAFS fitting was performed with S_0^2 fixed at 0.85. The shared fit parameters ΔE_0 and σ^2 were ΔE_0 = 2.6 (5) eV and σ^2 = 0.0072 (4) $Å^2$.

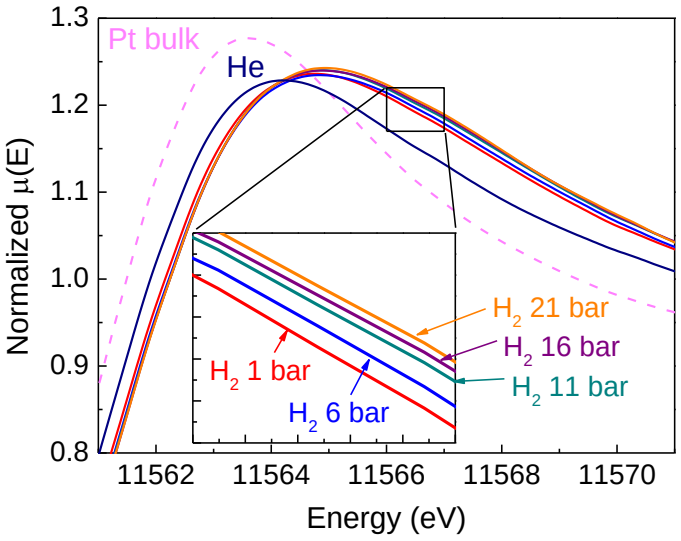

Fig. 1 Pressure dependent normalized absorption coefficient, μ(E), versus energy (XANES region) for the Pt-L_3 edge of Pt NPs on γ-Al_2O_3. Data were acquired at pressures from 1 bar to 21 bar at 25°C. Data acquired in He at 25°C and Pt foil data are also plotted for reference.

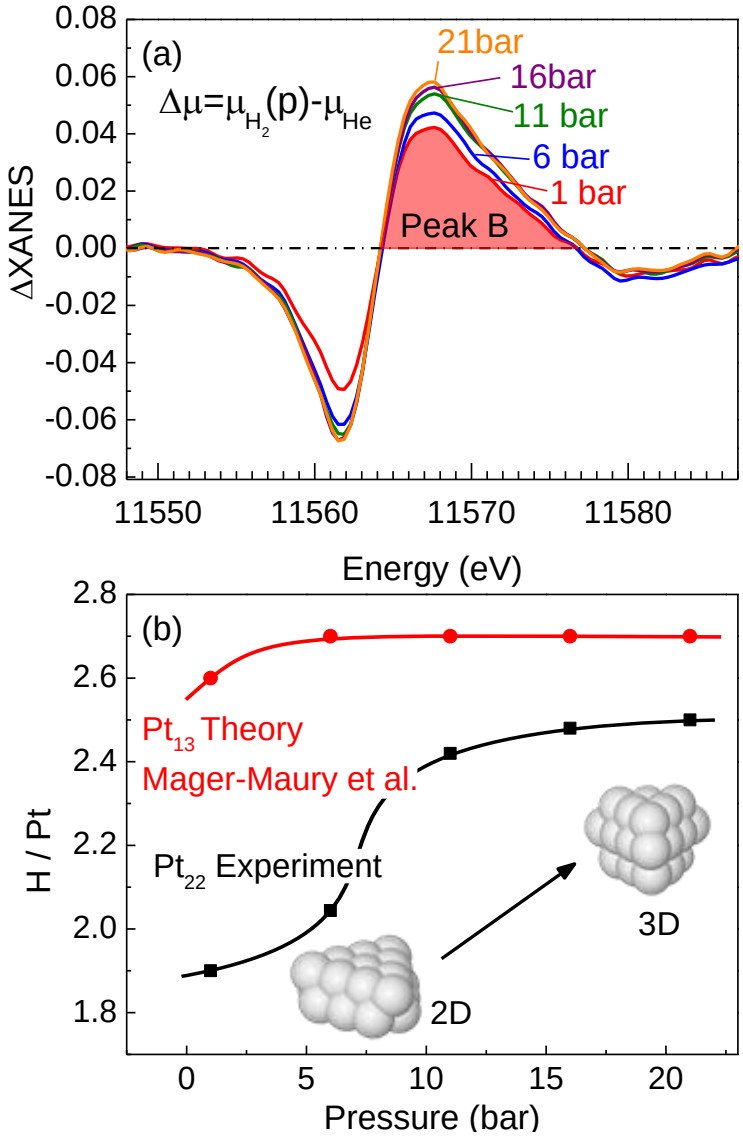

Fig. 2 (a) Difference XANES spectra (ΔXANES) from the Pt-L_3 absorption edge of Pt NPs on γ-Al_2O_3 displayed as a function of the H_2 pressure during measurement. In all plots, the RT He data are subtracted from those acquired at varying pressures in H_2. (b) H/Pt ratio calculated from the area of the ΔXANES peak B normalized by the area of bulk-like NPs measured at 183 K (black squares). Model shapes for low and high coverage are shown. Also plotted are theoretical H/Pt ratios from Mager-Maury et al. for Pt_{13} NPs (red circles).

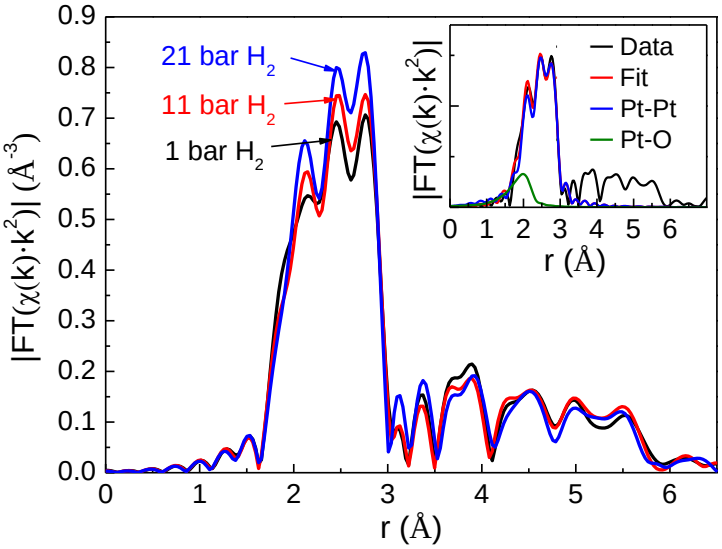

Fig. 3 Fourier transform magnitudes of k^2-weighted EXAFS for Pt/γ-Al_2O_3 NPs measured at 25°C under 1-21 bar H_2 pressure. A first shell fit of the experimental data measured under 11 bar H_2 is included as an inset.

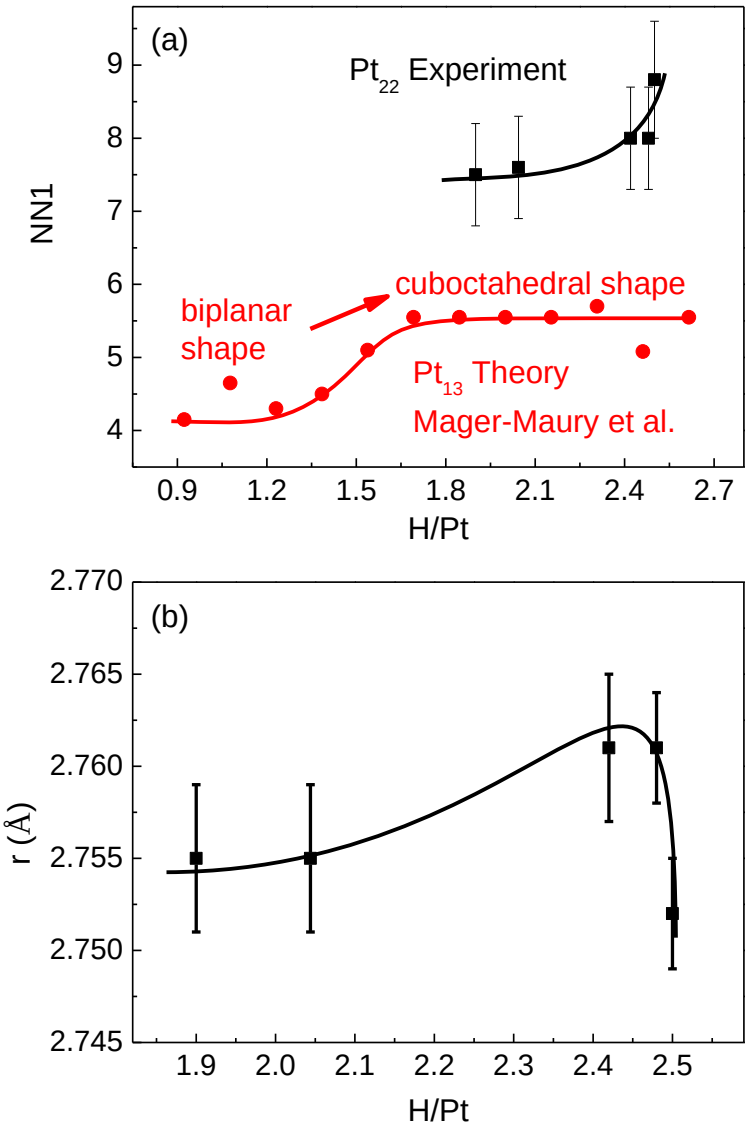

Fig. 4 (a) Pt-Pt first nearest-neighbor coordination number (NN1) from EXAFS single scattering analysis as a function of H coverage (black squares) and theoretical NN1 for Pt_{13} from Mager-Maury et al. (red circles). (b) Pt-Pt bond distance (r) as a function of H coverage (black squares).

References:

[1] a) F. Zaera, *Phys. Chem. Chem. Phys.* **2013**; b) P. Rylander, *Catalytic Hydrogenation over Platinum Metals*, Academic Press, **1967**.

[2] a) C. Cui, M. Ahmadi, F. Behafarid, L. Gan, M. Neumann, M. Heggen, B. Roldan Cuenya, P. Strasser, *Faraday Discuss.* **2013**; b) A. Wieckowski, E. R. Savinova, C. G. Vayenas, *Catalysis and Electrocatalysis at Nanoparticle Surfaces*, CRC Press, **2003**.

[3] a) Y. Li, R. T. Yang, *J. Phys. Chem. C* **2007**, *111*, 11086-11094; b) L. Wang, R. T. Yang, *J. Phys. Chem. C* **2008**, *112*, 12486-12494.

[4] a) S. Mukerjee, *J Appl Electrochem* **1990**, *20*, 537-548; b) M. Yamauchi, H. Kobayashi, H. Kitagawa, *ChemPhysChem* **2009**, *10*, 2566-2576; c) B. Roldan Cuenya, *Thin Solid Films* **2010**, *518*, 3127-3150; d) M. Vaarkamp, J. T. Miller, F. S. Modica, D. C. Koningsberger, *J. Catal.* **1996**, *163*, 294-305.

[5] C. Zhou, J. Wu, A. Nie, R. C. Forrey, A. Tachibana, H. Cheng, *J. Phys. Chem. C* **2007**, *111*, 12773-12778.

[6] a) F. Behafarid, L. Ono, S. Mostafa, J. Croy, G. Shafai, S. Hong, T. Rahman, S. R. Bare, B. Roldan Cuenya, *Phys. Chem. Chem. Phys.* **2012**, *14*, 11766-11779; b) M. K. Oudenhuijzen, J. A. van Bokhoven, J. T. Miller, D. E. Ramaker, D. C. Koningsberger, *J. Am. Chem. Soc.* **2005**, *127*, 1530-1540; c) C. Mager-Maury, G. Bonnard, C. Chizallet, P. Sautet, P. Raybaud, *ChemCatChem* **2011**, *3*, 200-207.

[7] L. Spenadel, M. Boudart, *J. Phys. Chem.* **1960**, *64*, 204-207.

[8] a) B. Kip, F. Duivenvoorden, D. Koningsberger, R. Prins, *J. Catal.* **1987**, *105*, 26-38; b) J. Singh, R. C. Nelson, B. C. Vicente, S. L. Scott, J. A. van Bokhoven, *Phys. Chem. Chem. Phys.* **2010**, *12*, 5668-5677; c) E. Bus, J. A. van Bokhoven, *Phys. Chem. Chem. Phys.* **2007**, *9*, 2894-2902.

[9] a) P. S. Petkov, G. P. Petrova, G. N. Vayssilov, N. Rösch, *J. Phys. Chem. C* **2010**, *114*, 8500-8506; b) A. Vargas, G. Santarossa, A. Baiker, *J. Phys. Chem. C* **2011**, *115*, 10661-10667; c) X. Liu, H. Dilger, R. Eichel, J. Kunstmann, E. Roduner, *J. Phys. Chem. B* **2006**, *110*, 2013-2023.

[10] a) C. H. Hu, C. Chizallet, C. Mager-Maury, M. Corral-Valero, P. Sautet, H. Toulhoat, P. Raybaud, *J. Catal.* **2010**, *274*, 99-110; b) Y. Lei, J. Jelic, L. C. Nitsche, R. Meyer, J. Miller, *Top. Catal.* **2011**, *54*, 334-348; c) S. I. Sanchez, L. D. Menard, A. Bram, J. H. Kang, M. W. Small, R. G. Nuzzo, A. I. Frenkel, *J. Am. Chem. Soc.* **2009**, *131*, 7040-7054.

[11] a) G. Rupprechter, H.-J. Freund, *Top. Catal.* **2000**, *14*, 3-14; b) L. Chen, C.-g. Zhou, J.-p. Wu, H.-s. Cheng, *Front. Phys. China* **2009**, *4*, 356-366.

[12] a) M. W. Small, S. I. Sanchez, N. S. Marinkovic, A. I. Frenkel, R. G. Nuzzo, *ACS Nano* **2012**, *6*, 5583-5595; b) C. Jensen, D. Buck, H. Dilger, M. Bauer, F. Phillipp, E. Roduner, *Chem. Commun.* **2013**, *49*, 588-590.

[13] a) Y. Ji, V. Koot, A. M. van der Eerden, B. M. Weckhuysen, D. C. Koningsberger, D. E. Ramaker, *J. Catal.* **2007**, *245*, 415-427; b) N. Guo, B. R. Fingland, W. D. Williams, V. F. Kispersky, J. Jelic, W. N. Delgass, F. H. Ribeiro, R. J. Meyer, J. T. Miller, *Phys. Chem. Chem. Phys.* **2010**, *12*, 5678-5693; c) O. S. Alexeev, F. Li, M. D. Amiridis, B. C. Gates, *J. Phys. Chem. B* **2005**, *109*, 2338-2349; d) T. Kubota, K. Asakura, N. Ichikuni, Y. Iwasawa, *Chem. Phys. Lett.* **1996**, *256*, 445-448; e) D. Ramaker, D. Koningsberger, *Phys. Chem. Chem. Phys.* **2010**, *12*, 5514-5534; f) S. N. Reifsnyder, M. M. Otten, D. E. Sayers, H. H. Lamb, *J. Phys. Chem. B* **1997**, *101*, 4972-4977; g) S. Bordiga, E. Groppo, G. Agostini, J. A. van Bokhoven, C. Lamberti, *Chem. Rev.* **2013**, *113*, 1736-1850; h) M. Teliska, W. O'Grady, D. Ramaker, *J. Phys. Chem. B* **2004**, *108*, 2333-2344.

[14] a) B. Roldan Cuenya, M. A. Ortigoza, L. Ono, F. Behafarid, S. Mostafa, J. Croy, K. Paredis, G. Shafai, T. Rahman, L. Li, *Phys. Rev. B* **2011**, *84*, 245438; b) B. Roldan Cuenya, J. R. Croy, S.

Mostafa, F. Behafarid, L. Li, Z. Zhang, J. C. Yang, Q. Wang, A. I. Frenkel, *J. Am. Chem. Soc.* **2010**, *132*, 8747-8756.
[15] A. Y. Stakheev, Y. Zhang, A. Ivanov, G. Baeva, D. Ramaker, D. Koningsberger, *J. Phys. Chem. C* **2007**, *111*, 3938-3948.
[16] a) K. Paredis, L. K. Ono, F. Behafarid, Z. Zhang, J. C. Yang, A. I. Frenkel, B. R. Cuenya, *J. Am. Chem. Soc.* **2011**, *133*, 13455-13464; b) Y. Zhang, M. L. Toebes, A. van der Eerden, W. E. O'Grady, K. P. de Jong, D. C. Koningsberger, *J. Phys. Chem. B* **2004**, *108*, 18509-18519; c) A. Y. Stakheev, Y. Zhang, A. Ivanov, G. Baeva, D. Ramaker, D. Koningsberger, *The Journal of Physical Chemistry C* **2007**, *111*, 3938-3948; d) L. R. Merte, M. Ahmadi, F. Behafarid, L. K. Ono, E. Lira, J. Matos, L. Li, J. C. Yang, B. Roldan Cuenya, *ACS Catal.* **2013**, 130517100016006.
[17] M. Di Vece, D. Grandjean, M. Van Bael, C. Romero, X. Wang, S. Decoster, A. Vantomme, P. Lievens, *Phys. Rev. Lett.* **2008**, *100*.
[18] M. Hakamada, T. Furukawa, T. Yamamoto, M. Takahashi, M. Mabuchi, *Mater. Trans.* **2011**, *52*, 806-809.
[19] E. Bus, J. T. Miller, A. J. Kropf, R. Prins, J. A. van Bokhoven, *Phys. Chem. Chem. Phys.* **2006**, *8*, 3248-3258.
[20] S. R. Bare, N. Yang, S. D. Kelly, G. E. Mickelson, F. S. Modica, *Catal. Today* **2007**, *126*, 18-26.
[21] M. Newville, *Journal of synchrotron radiation* **2001**, *8*, 322-324.
[22] B. Ravel, M. Newville, *Journal of synchrotron radiation* **2005**, *12*, 537-541.